

Dual Probe with Fluorescent and Magnetic Properties for Imaging Solid Tumor Xenografts

Liang Shan, Songping Wang, Rajagopalan Sridhar, Zaver M. Bhujwalla, and Paul C. Wang

Abstract

A dual probe with fluorescent and magnetic reporter groups was constructed by linkage of the near-infrared (NIR) fluorescent transferrin conjugate (Tf^{NIR}) on the surface of contrast agent–encapsulated cationic liposome (Lip-CA). This probe was used for magnetic resonance imaging (MRI) and optical imaging of MDA-MB-231-luc breast cancer cells grown as a monolayer *in vitro* and as solid tumor xenografts in nude mice. Confocal microscopy, optical imaging, and MRI showed a dramatic increase of *in vitro* cellular uptake of the fluorescent and magnetic reporter groups from the probe compared with the uptake of contrast agent or Lip-CA alone. Pretreatment with transferrin (Tf) blocked uptake of the probe reporters, indicating the importance and specificity of the Tf moiety for targeting. Intravenous administration of the dual probe to nude mice significantly enhanced the tumor contrast in MRI, and preferential accumulation of the fluorescent signal was clearly seen in NIR-based optical images. More interestingly, the contrast enhancement in MRI showed a heterogeneous pattern within tumors, which reflected the tumor's morphologic heterogeneity. These results indicate that the newly developed dual probe enhances the tumor image contrast and is superior to contrast agent alone for identifying the tumor pathologic features on the basis of MRI but also is suitable for NIR-based optical imaging.

TUMOR IMAGING exploits the differences in physical properties between malignant and normal tissues. These differences are often insufficient for good contrast resolution.^{1–3} Contrast-enhanced magnetic resonance imaging (MRI) is one of the best noninvasive methodologies available today in clinical medicine for assessing the anatomy and function of tissues.⁴ High spatial resolution and high soft tissue contrast are desirable features of noninvasive MRI. However, owing to intrinsically low sensitivity, high local concentration of contrast agents (CAs) is required to generate detectable magnetic resonance contrast. A large amount of CA has to be used owing to the nonspecific uptake by tumors and other

tissues *in vivo*. In recent years, targeted CA delivery systems have been developing based on the concept that molecular imaging can increase the signal to noise ratio by detecting differences in ‘molecular properties’ between cancer and normal tissues.^{5–7} This should, in theory, allow for detection of smaller tumors. As one strategy, monoclonal antibodies or antibody fragments have been coupled with CA directly or linked with CA through liposome (Lip) carrier. However, insufficient direct linkage of gadolinium (Gd) with antibody or the relatively large molecular size of antibody-Lip-Gd particles may limit its use as a CA for imaging cell surface receptors in solid tumors because of inefficient extravasation and very slow diffusion in the interstitial compartment.^{2,8,9} Furthermore, antibody immunogenicity, poor stability of the conjugates, and potential change of the antibody binding ability owing to changes in surface antigens are still problematic for *in vivo* application. A ligand with less toxic, high binding specificity for tumors and relatively small size and without immunogenicity is required to target the CA to tumors.

Optical imaging offers several advantages over other imaging techniques. Among these are the simplicity of the technique, high sensitivity, and absence of ionizing radiation. There is increasing interest in the development of techniques for *in vivo* evaluation of gene expression, monitoring of gene delivery, and real-time intraoperative

From the Departments of Radiology and Radiation Oncology, Howard University, Washington, DC; and Department of Radiology, Johns Hopkins University School of Medicine, Baltimore, MD.

This study was made possible by grant number 2G12RR003048 from the National Center for Research Resources, a component of the National Institutes of Health (NIH). It was also supported by the following grants: USAMRMC W81XWH-05-1-0291, DAMD17-00-1-0291, DAMD17-03-1-0759, and NIH 5U54CA091431.

Address reprint requests to: Paul C. Wang, PhD, Department of Radiology, Howard University, 2041 Georgia Avenue, NW, Washington, DC 20060; e-mail: pwang@howard.edu.

DOI 10.2310/7290.2007.00006

© 2007 BC Decker Inc

visualization of tumor margins and metastatic lesions to improve surgical outcome.^{10–12} Limited depth of light penetration and a lack of tomographic information prevent *in vivo* efficiency of optical imaging. To overcome the limitations of various imaging modalities, multimodal probes have been developed for detection using multiple imaging devices.^{13–15}

Transferrin receptor (TfR) is a cell surface internalizing receptor that is responsible for almost all iron sequestration in mammalian cells. TfR is overexpressed in 74% of breast carcinomas, 76% of lung adenocarcinomas, and 93% of lung squamous cell carcinomas. The expression level of TfR receptor is of great value in grading tumors and determining prognosis.^{16,17} TfR has been successfully applied as a molecular target to direct therapeutic agents to tumor cells.¹⁷ Transferrin (Tf), the TfR ligand, is a monomeric glycoprotein that binds Fe³⁺ for delivery to vertebrate cells through receptor-mediated endocytosis. Fluorescently labeled Tf has greatly aided the investigation of endocytosis *in vitro*. Tf has also been successfully used in targeted gene therapy *in vivo*.^{18,19} We hypothesized that near-infrared (NIR) dye-labeled Tf (Tf^{NIR}) would be an ideal ligand for targeting MRI and optical reporters to solid tumors, enabling better contrast-enhanced MRI and NIR-based optical detection. We developed a Tf- and Lip-mediated dual molecular probe with both fluorescent and magnetic reporter groups. The Tf^{NIR} was linked on the surface of Lip particles, whereas the MRI CA (Magnevist, obtained from Berlex Laboratories, Wayne, NJ) was encapsulated within the Lip. These components conjugated together and formed small uniform vesicles (less than 100 nm in diameter). *In vitro* analysis demonstrated that the probe dramatically improved the uptake of CA and NIR dye in monolayer cultures of MDA-MB-231-luc human breast cancer cells through both receptor- and Lip-mediated endocytosis. *In vivo*, the probe significantly enhanced the magnetic resonance signals from the MDA-MB-231-luc cells grown as solid tumor xenografts in nude mice and was superior to the CA alone for identifying the tumor morphology and infrastructure. Simultaneously, a significant preferential accumulation of fluorescent signal by the tumors was clearly detectable in Tf^{NIR}-based optical imaging.

Materials and Methods

Materials

Cationic lipids including 1,2-dioleoyl-sn-glycero-3-phosphoethanolamine (DOPE), 1,2-dioleoyl-3-trimethylammo-

nium-propane (DOTAP), and fluorescent lipid DOPE-N-(7-nitro-2-1,3-benzoxadiazole-4-yl) (NBD-DOPE) were purchased from Avanti Polar Lipids (Alabaster, AL). They were premixed and dissolved in chloroform in a formula of DOTAP:DOPE (1:1 w/w) (Lip) or in a fluorescent formula of DOTAP:DOPE + 0.1% NBD-DOPE (Lip^{NBD}). Fluorescent Alexa fluor 680 conjugate of human Tf (Tf^{NIR}), a SelectFX nuclear labeling kit, Alexa fluor 680 fluorophore, and enzyme-free phosphate-buffered saline (PBS)-based cell dissociation solution were purchased from Invitrogen (Carlsbad, CA). Holo-transferrin without fluorescent conjugate and MicroSpin G-50 columns were obtained from Sigma (St. Louis, MO) and Amersham Biosciences (Piscataway, NJ), respectively. The SPI-Pore polycarbonate membrane filter and filter holder were from Structure Probe Inc (West Chester, PA).

Preparation of the Molecular Dual Probe: Tf^{NIR}-Lip^{NBD}-CA Complex

The Tf^{NIR}-Lip^{NBD}-CA complex was constructed using Tf^{NIR}, cationic Lip^{NBD}, and Magnevist. Premixed Lip^{NBD} in chloroform (3.607 μ L) was dried under a nitrogen stream and hydrated by adding 50 μ L of water containing 12 μ L of Magnevist. Each microliter of Magnevist contains 469.01 μ g of gadopentatate dimeglumine. The hydrated Lip^{NBD}-CA mixture was homogenized using a vortex generator and incubated for 10 minutes. The volume of the mixture was adjusted to 175 μ L with water. The mixture was then sequentially downsized by sonication (80–90 W, 10 minutes) in a water bath and by repeatedly passing through polycarbonate filters with decreasing pore diameter 0.2/0.1 μ m. Following that, 25 μ L of Tf^{NIR} (5 mg/mL) was mixed and incubated for at least 10 minutes. Gel filtration through a Sephadex G-50 column was used to remove unencapsulated CA and free Tf^{NIR}. A freshly prepared probe was used in all analysis. The final volume was 200 μ L, and Lip:Tf:Magnevist composition was 10:12.5:0.56 (nmol/ μ g/mg). To monitor different components of the probe, nonfluorescent Tf and Lip were used instead of fluorescent Tf^{NIR} and Lip^{NBD} in some experiments.

Cell Culture and Animal Model

The MDA-MB-231-luc human breast cancer cell line (Xenogen, Alameda, CA) was used to test the efficiency of the probe *in vitro* and *in vivo*. This cell line is well documented for constitutional overexpression of TfR and has been transfected with the luciferase gene for luciferase-

based optical imaging. (In this study, we did not use luciferase-based imaging.) Cells were routinely maintained in Dulbecco's Modified Eagle's Medium/F-12 medium supplemented with 10% heat-inactivated fetal bovine serum (FBS) and 50 $\mu\text{g}/\text{mL}$ each of penicillin, streptomycin, and neomycin (Invitrogen). The solid tumor xenograft model was developed by subcutaneous injection of 1×10^7 subconfluent cells in 100 μL Dulbecco's phosphate-buffered saline (DPBS) in the lower back of female athymic nude mice (8–10 weeks old; Harlan, Indianapolis, IN). The probe was evaluated in a total of 10 nude mice bearing tumors from 0.4 to 1.2 cm in diameter.

Confocal Microscopy

Tumor cells were grown on eight-chamber glass slides. Twenty-four hours later, the cells at 40 to 50% confluence were incubated with 25 μL of one of the following probes in 150 μL of medium without FBS and antibiotics. The probes included Tf^{NIR}-Lip^{NBD}-CA, Tf-Lip^{NBD}-dye, and dye alone. To visualize the cellular uptake of probe reporters, an NIR dye Alexa fluor 680 fluorophore was used to replace the CA in the preparation of Tf-Lip^{NBD}-dye probe at a concentration of 2 μL in a 200 μL total probe. Incubation was carried out for 5, 30, 60, and 120 minutes, separately. After PBS washing (three times), cells were fixed using 10% neutralized formalin for 10 minutes and cell nuclei were counterstained using 4',6-diamidino-2-phenylindole dihydrochloride (DAPI) blue-fluorescence dye. Confocal images were acquired with a Zeiss LSM 510 Confocal Microscopy System (Carl Zeiss Inc, Thornwood, NY) using a 633 nm excitation line and emission LP 650 filter for Tf^{NIR} and Alexa fluor 680 fluorophore (red), 488 nm excitation line and emission BP 505 – 550 filter for Lip^{NBD} (green), and 364 nm excitation line and emission BP 385 – 470 filter for DAPI (blue). Following sequential excitation, red, green, and blue fluorescent images of the same cells were merged using the Zeiss AIM software for colocalization of the probe different reporters within cells.

In Vitro MRI and Optical Imaging

To quantify the cellular uptake of probe reporters, optical imaging and MRI of the cell pellets were performed. Similar numbers of tumor cells were seeded on 10 cm culture dishes for optical imaging and in 150 cm flasks for MRI. Cells grown to subconfluence were incubated with a 200 μL probe (in 3 mL medium) for 10 cm dishes and a 600 μL probe (in 10 mL medium) for 150 cm flasks.

Differently labeled probes, such as Tf^{NIR}-Lip^{NBD}-CA, Tf-Lip^{NBD}-dye, Lip^{NBD}-dye, CA alone, and dye alone, were used. Incubation was carried out for 60 minutes. After PBS washing (three times), cells were collected using enzyme-free cell dissociation solution and adjusted to the same number. Cells were pelleted in microcentrifuge tubes by centrifugation. The cell pellets were quantified with respect to fluorescent intensity (FI) using the Xenogen IVIS 200 imaging system with excitation/emission filters at 679/702 nm for Tf^{NIR} and the Alexa fluor 680 fluorophore and at 464/531 nm for Lip^{NBD} measurement. Statistical analysis (Student's two-tailed *t*-test) of the FI for cells with different treatments was performed using Microsoft Excel. To obtain enough cells for MRI, cell pellets were pooled from five replicates. MRI was acquired using a Bruker 400 MHz NMR machine (Bruker-Biospin, Billerica, MA). A spin-echo (SE) imaging sequence was used to obtain T₁-weighted images. The imaging parameters were as follows: echo time (TE) = 11.416 milliseconds, repetition time (TR) = 500 milliseconds, number of averages = 4, field of view = 20 \times 20 mm, matrix size = 256 \times 128, and slice thickness = 2 mm. A fast imaging with steady-state precession sequence was used for T₁ measurement. The T₁ measurement parameters were as follows: TE = 1.5 milliseconds, TR = 3 milliseconds, number of averages = 8, number of frames = 16, number of segments = 32, inversion delay = 49.2 milliseconds, and inversion repetition = 2572.3 milliseconds. The MRIs were taken in the cross-sectional view of the microcentrifuge tubes. The central slice image, which was not influenced by the image distortion owing to the susceptibility effect from the air-pellet boundary, was used for signal intensity measurement. All analyses were performed using the Bruker image sequence analysis tools. All experiments were repeated at least three times. The representative data are presented.

In Vivo MRI and Optical Imaging

The animal was anesthetized using 2% isoflurane and positioned with the tumor at the center of the coil. The physiologic condition of the animals was monitored using a respiratory gating device during the scanning. The tumor was scanned in the perpendicular direction of the tumor and animal skin interface using a Bruker 400 MHz, 89 mm NMR spectrometer. After a search for overall image quality, imaging time, and probe- and CA-mediated contrast enhancement using different imaging sequences and parameters, a multislice multiecho T₁-weighted SE sequence was used for imaging studies, with a TR of 800 milliseconds, a TE of 11.4 milliseconds, and a slice

thickness of 1 mm. For each animal, a baseline image was first obtained; the tumors were then sequentially imaged at an interval of 10 minutes until 3 hours following intravenous injection of 200 μL of Tf^{NIR} -Lip^{NBD}-CA probe (containing 12 μL of Magnevist) through the tail vein. This was equivalent to two times the Magnevist dosage used in the clinic. For comparative study, the same animals were also imaged following intravenous administration of the same dosage of Lip-CA and CA alone (12 μL of Magnevist in 200 μL of pure water). The interval period between the two MRI studies was at least 3 days to avoid any influence of CA from the previous imaging study. The direction of the tumor was marked each time with water-filled small balls and marker pens before imaging. For optical imaging, the FI of tumors was monitored from 10 minutes after administration of the probe to 3 to 5 days using a Xenogen IVIS 200 imaging system.

Pathologic Analysis

After imaging, the mice were autopsied and the tumors were sampled, fixed in 10% neutral buffered formalin, and embedded in paraffin. Tumors were sectioned in the same direction as MRIs based on the markers of the tumor border made before MRI. Hematoxylin-eosin staining was used for pathologic examination. A comparison was performed between the tumor pathology and the image enhancement pattern in MRI.

Results

Visualization of Tf- and Lip-Mediated Cellular Uptake

For confocal microscopic observation of the cellular uptake of the probe reporters, cells were incubated with the probe Tf -Lip^{NBD}-dye or dye alone from 5 minutes to 2 hours. Here the probe was constructed using unlabeled Tf and NIR fluorescent dye instead of CA to visualize the uptake of encapsulated reagents within Lip. Figure 1 shows representative microscopic images. Both Lip^{NBD} (green) and fluorescent dye (red) were observed to be present in the cell cytoplasm as early as 5 minutes after incubation with the probe, and their FI within the cytoplasm increased gradually, reaching a maximum at about 1 hour of incubation (see Figure 1, A–C). Interestingly, the Lip^{NBD} and dye accumulated again, forming multiple endosomes. These endosomes were mainly located at the peripheral area of the cytoplasm and became more evident at 2 hours of incubation (see Figure 1, D–F), suggesting receptor-

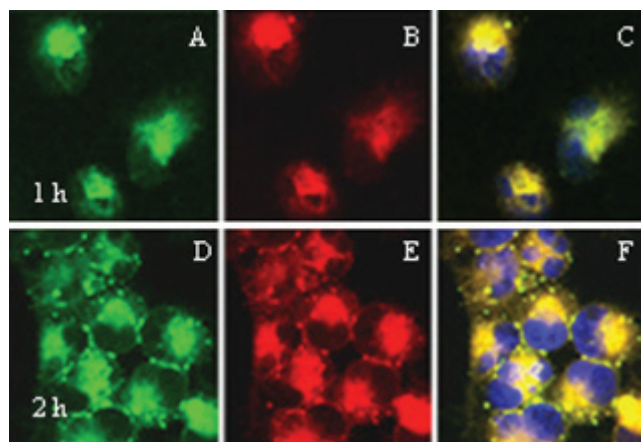


Figure 1. Confocal microscopic observation of cellular uptake of probe reporters. Cells were incubated with the probe transferrin-liposome-nitrobenzoxadiazole (Tf -Lip^{NBD})-dye for 5 minutes to 2 hours. A to C are representative images acquired at the 1 hour of incubation time point showing distribution and colocalization of Lip^{NBD} (A) and near-infrared (NIR) dye (B) in the cytoplasm. D to F are representative images acquired at the 2 hours of incubation time point showing multiple endosomes formed by Lip (D) and NIR dye (E) and colocalized in the peripheral area of the cytoplasm (F). Nuclei were counterstained using 4',6-diamidino-2-phenylindole dihydrochloride (DAPI). Cells were imaged with a 63×1.4 NA Plan-Apochromat oil-immersion objective.

mediated endocytosis and release or degradation of the probe reporters through the action of lysosomal enzymes. Cellular uptake of the dye was not evident in the cells incubated with dye alone.

To visualize whether the Tf and Lip were co-internalized, confocal microscopy and optical imaging were performed for cells incubated with Tf^{NIR} -Lip^{NBD}-CA, Lip^{NBD}-CA, or CA alone. Similarly, from 5 minutes of incubation, the Tf^{NIR} (Figure 2A) and Lip^{NBD} (Figure 2B) were already colocalized within cell cytoplasm (Figure 2C). Optical imaging of the cell pellets further confirmed the uptake of the probe in tumor cells. To avoid membrane damage and probe leakage from cells, enzyme-free PBS-based cell dissociation solution was used instead of trypsin for cell dissociation from culture dishes. As shown in Figure 2D, only cells incubated with Tf^{NIR} -Lip^{NBD}-CA showed a strong fluorescent signal of Tf^{NIR} . Both cells incubated with Tf^{NIR} -Lip^{NBD}-CA and cells incubated with Lip^{NBD}-CA showed strong fluorescent signal of Lip^{NBD} (Figure 2E). Neither Tf^{NIR} nor Lip^{NBD} signal was detectable in cells incubated with CA alone.

We further evaluated whether the CA encapsulated within the probe was internalized into tumor cells using MRI of the cell pellets. A representative MRI of the cell pellets obtained from cells incubated with Tf^{NIR} -Lip^{NBD}-

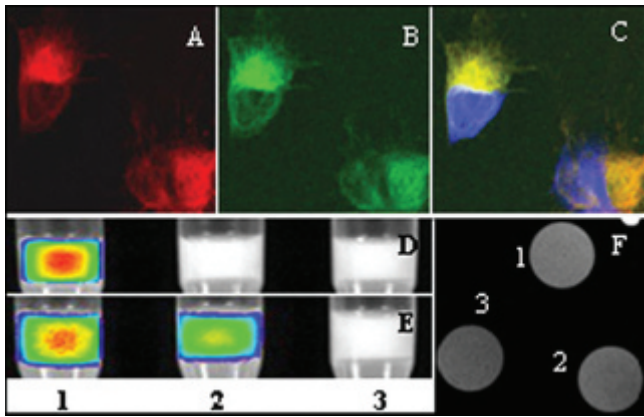


Figure 2. Confocal, optical, and magnetic resonance imaging (MRI) detection of the reporters in cells incubated with the probe near-infrared transferrin-liposome-nitrobenzoxadiazole-contrast agent (Tf^{NIR} -Lip^{NBD}-CA) for 1 hour. A to C are representative confocal microscopic images showing distribution and colocalization of Tf^{NIR} (A) and Lip^{NBD} (B) in cytoplasm. D to E are optical images of the cell pellets. A strong fluorescent signal of Tf is detected in cells incubated with Tf^{NIR} -Lip^{NBD}-CA (D, lane 1) but not in cells incubated with Lip^{NBD}-CA or with CA alone (D, lanes 2 and 3). Similarly, the strongest signal of Lip^{NBD} is detected in cells incubated with Tf^{NIR} -Lip^{NBD}-CA (E, lane 1) and less in cells incubated with Lip^{NBD}-CA (E, lane 2) but not in cells incubated with CA alone (E, lane 3). F shows the MRIs of the cell pellets. A stronger signal enhancement and T_1 shortening are obtained in cells incubated with Tf^{NIR} -Lip^{NBD}-CA and in cells incubated with Lip^{NBD}-CA (1 and 2) than in cells incubated with CA alone (3). The MRI parameters are as follows: echo time = 11.416 milliseconds, repetition time = 500 milliseconds, number of averages = 4, field of view = 20×20 mm, matrix size = 256×128 , and slice thickness = 2 mm.

CA, Lip^{NBD}-CA, or CA alone is shown in Figure 2F. The corresponding signal intensity and T_1 relaxation time are shown in Table 1. Cells incubated with the probe Tf^{NIR} -Lip^{NBD}-CA or Lip^{NBD}-CA showed a much greater positive

contrast and T_1 shortening than the cells incubated with CA alone. The T_1 relaxation time shortened from 408 milliseconds for CA alone to 374 milliseconds for Lip^{NBD}-CA and 366 milliseconds for Tf^{NIR} -Lip^{NBD}-CA ($p < .05$). The cells incubated with Tf^{NIR} -Lip^{NBD}-CA also showed higher signal intensity than the cells incubated with Lip^{NBD}-CA. These results highly indicate the importance and specificity of Tf moiety for targeting the probe internalization into tumor cells in vitro. The difference in signal intensity and T_1 relaxation time mediated by Lip^{NBD}-CA and by CA alone might reflect the effective fusion of Lip with tumor cell membrane.

Quantification of Tf- and Lip-Mediated Cellular Uptake

To evaluate the efficiency of Tf- and Lip-mediated cellular uptake, the FI of the Lip^{NBD} and NIR dye within the tumor cells was quantified following 1 hour's incubation of the cells with probes. The FI of NIR dye in the cells incubated with Tf-Lip^{NBD}-dye and with Lip^{NBD}-dye was more than 200-fold higher than that in the cells with dye alone (Table 2). Cells incubated with dye alone showed a similar level of FI to cells without probe and dye exposure (autofluorescence background). Approximately 1.5-fold higher FI of the intracellular NIR dye was observed in cells incubated with Tf-Lip^{NBD}-dye than in cells incubated with Lip^{NBD}-dye. Similarly, 2-fold higher FI of Lip^{NBD} was detected in cells incubated with Tf-Lip^{NBD}-dye or Lip^{NBD}-dye than in cells incubated with NIR dye alone (autofluorescent background) (see Table 2). The FI of Lip^{NBD} was 1.3-fold higher in cells incubated with Tf-Lip^{NBD}-dye than in cells incubated with Lip^{NBD}-dye. Student's *t*-tests (two-tailed)

Table 1. Comparison between Probe- and Contrast Agent-Mediated Signal Enhancement

MRI Measurement	Tf^{NIR} -Lip ^{NBD} -CA	Lip ^{NBD} -CA	CA Alone
Relative intensity (10^5)	17.7 ± 0.86	15.33 ± 0.86	13.25 ± 0.78
T_1 relaxation time (ms)	366.7 ± 17.1	374.3 ± 17.3	408.1 ± 13.8

CA = contrast agent; Lip = liposome; NBD = nitrobenzoxadiazole; NIR = near-infrared; Tf = transferrin. $p < .05$ between probe and CA alone for both relative intensity and T_1 .

Table 2. Optical Quantitation of Probe-Mediated Cellular Uptake of Reporters

Reporters	Tf -Lip ^{NBD} -Dye	Lip ^{NBD} -Dye	Dye Alone
NIR dye ($\times 10^9$)	6.88 ± 0.59	4.99 ± 0.51	0.23 ± 0.006
Lip ^{NBD} ($\times 10^7$)	2.03 ± 0.14	1.64 ± 0.09	1.10 ± 0.13

Lip = liposome; NBD = nitrobenzoxadiazole; NIR = near-infrared; Tf = transferrin. $p < .05$ between probe and dye alone and also between Tf-Lip^{NBD} dye and Lip^{NBD} dye for both dye and Lip^{NBD} uptake. Quantitation is based on the fluorescence intensity (p/s/cm²/sr) of cell pellets.

between cells incubated with probe and with dye alone for both intracellular Lip^{NBD} and NIR dye intensity were both significantly different ($p < .05$). The FI in cells incubated with Tf-Lip^{NBD}-dye and in cells incubated with Lip^{NBD}-dye was also significantly different ($p < .05$) for both intracellular Lip^{NBD} and NIR dye uptake.

To further test the specificity of Tf-mediated cellular uptake, cells were first pretreated for 1 hour with unlabeled Tf before incubation with the probes. The amount of Tf was threefold (375 $\mu\text{g}/\text{dish}$) higher than that used in the probe (125 $\mu\text{g}/\text{dish}$). Following incubation with the probe Tf-Lip^{NBD}-dye, the FI of the NIR dye in cells with and without Tf pretreatment was 2.45×10^9 and 3.42×10^9 p/s/cm²/sr, respectively (Table 3). The FI of the Lip^{NBD} in cells with and without Tf pretreatment was 2.57×10^7 and 3.45×10^7 p/s/cm²/sr, respectively. Calculation based on the control cells incubated with Lip^{NBD}-dye revealed a blockage of 65.6% of the dye uptake and 70.97% of the Lip^{NBD} uptake by Tf pretreatment. These results indicate that the probe reporter uptake in vitro was mediated by both Tf and cationic Lip. Tf and Lip have an apparent synergistic effect on the cellular uptake of the probe reporters.

Probe-Mediated Signal Enhancement of the Tumors In Vivo

Signal enhancement was evaluated in 10 athymic nude mice with solid tumor xenografts. The tumor size ranged from 0.4 to 1.2 cm in diameter. To compare the signal enhancement mediated by the probe and mediated by the CA alone, the same mice were used for the probe and CA-alone studies sequentially with an interval of at least 3 days. Intravenous administration of the probe Tf^{NIR}-Lip^{NBD}-CA significantly enhanced the tumor image contrast (Figure 3). The enhancement was observed as early as 10 minutes after administration and increased gradually, reaching the maximum at 90 minutes to 2 hours. After that, a gradual decrease in the signal enhancement was observed. Interestingly, the enhancement was greatly heterogeneous within the tumors (see Figure 3). The enhancement

pattern became relatively consistent from 1 to 3 hours. Some areas of the tumors were strongly enhanced initially, whereas other areas were weakly enhanced. The signals from the strongly enhanced region decreased much more slowly than the signals from the region with weak enhancement. For small tumors, the enhancement was relatively uniform and the enhancement was usually observed starting from the peripheral area. Magnevist alone slightly enhanced the image contrast of tumors compared with the baseline images (Figure 4). The maximum enhancement was usually observed at 30 to 60 minutes after injection. The image contrast enhancement started from the peripheral area to the center of the tumors and was relatively uniform within tumors irrespective of the sizes studied here. The signal enhancement decreased rapidly and returned to baseline within 3 hours. The pharmacokinetics of pure Magnevist was different from that of Tf-labeled Magnevist containing Lip. Magnevist containing Lip without linkage to Tf showed a much weaker signal enhancement than either CA alone or Tf^{NIR}-Lip^{NBD}-CA.

Detection and Dynamic Change of the Fluorescent Signal in Tumors In Vivo

To understand whether the probe was preferentially accumulated in tumors and whether the fluorescent signal was optically detectable in vivo, tumors were monitored using Tf^{NIR}-based optical imaging. The fluorescent signal was clearly detectable as early as 10 minutes and reached the maximum intensity at about 90 minutes to 2 hours after intravenous injection of the probe Tf^{NIR}-Lip^{NBD}-CA (Figure 5). The FI was related to the tumor sizes, and significant FI was still detectable after 2 days for larger tumors (usually > 0.8 cm in diameter). The FI of smaller tumors became very weak at 24 hours. The FI of Lip^{NBD} was too weak to be detectable by optical imaging in vivo, although it was clearly detected ex vivo. High background fluorescence was another reason for the failure to detect Lip^{NBD} in tumors. Following intravenous injection, the probe was rapidly distributed throughout the body and

Table 3. Blockage of Transferrin-Mediated Uptake of Reporters by Transferrin Pretreatment

Reporters	Tf-Lip ^{NBD} -Dye	Tf-Lip ^{NBD} -Dye	Lip ^{NBD} -Dye
NIR dye ($\times 10^9$)	3.42 ± 0.17	2.45 ± 0.21	1.94 ± 0.20
Lip ^{NBD} ($\times 10^7$)	3.45 ± 0.29	2.57 ± 0.21	2.21 ± 0.16

Lip = liposome; NBD = nitrobenzoxadiazole; NIR = near-infrared; Tf = transferrin.

$p < .05$ between pretreated and untreated cells for both dye and Lip^{NBD} uptake. Quantitation is based on the fluorescence intensity (p/s/cm²/sr) of cell pellets.

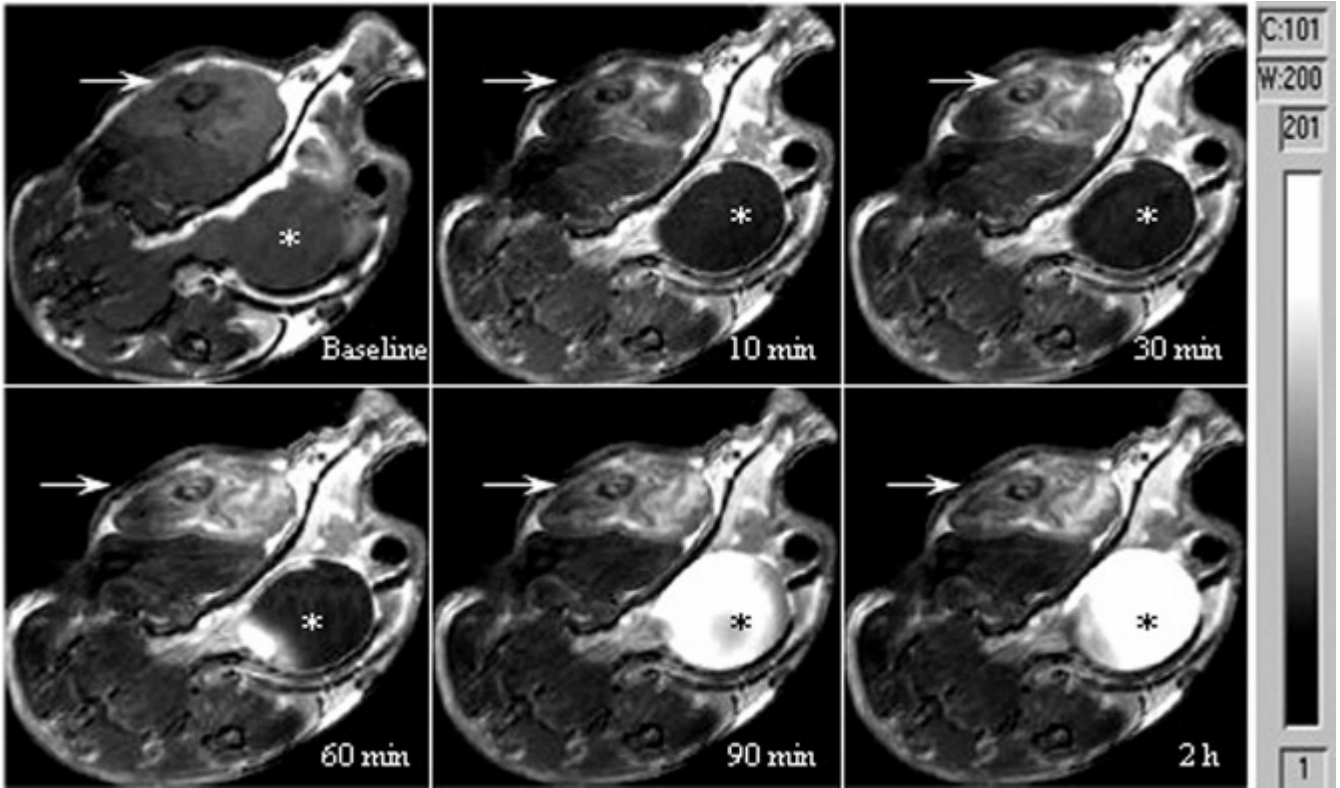


Figure 3. In vivo time course of tumor magnetic resonance imaging (MRI) after intravenous administration of the probe transferrin-liposome-nitrobenzoxadiazole-contrast agent ($\text{Tf}^{\text{NIR}}\text{-Lip}^{\text{NBD}}\text{-CA}$) showing gradually increased enhancement of the tumor signal (*arrow*) and a heterogeneous enhancement pattern. Gradual accumulation of contrast agent in the urinary bladder is evident (*). The MRI parameters are as follows: echo time = 11.416 milliseconds, repetition time = 800 milliseconds, number of averages = 4, field of view = 28×30 mm, matrix size = 256×192 , and slice thickness = 1.0 mm.

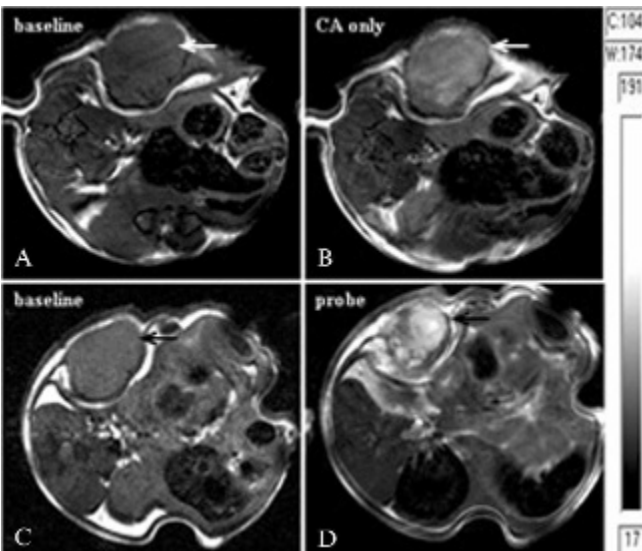


Figure 4. Comparison of the signal enhancement by contrast agent (CA) alone (A–B) and by the probe transferrin-liposome-nitrobenzoxadiazole-contrast agent ($\text{Tf}^{\text{NIR}}\text{-Lip}^{\text{NBD}}\text{-CA}$) (C–D). The magnetic resonance images (MRIs) are from the same tumor, with an interval of 72 hours between studies with the probe and with CA alone. A stronger, heterogeneous signal enhancement is achieved with $\text{Tf}^{\text{NIR}}\text{-Lip}^{\text{NBD}}\text{-CA}$ over CA alone. The MRI parameters are the same as for Figure 3.

was first taken up by the well-perfused organs, such as the liver, spleen, lung, and bone marrow. However, the probe was rapidly washed out from these organs but not from solid tumors. The uptake of the probe in tumors was enhanced because of binding to TfR in the tumor. After the initial rapid increase in the background fluorescence following injection of the probe, the background fluorescence decreased rapidly, as shown in Figure 5H. The tumor to normal (contralateral muscle) ratio varied from 1.3 to 3.4 at the different time points following injection (from 10 minutes to 48 hours), which was related to the tumor sizes. Small tumors (less than 3 mm in diameter) showed less fluorescent signal, perhaps owing to differences in vasculature. Similar to the MRI finding, fluorescent dye containing Lip without Tf linkage failed to induce a preferential increase in fluorescent signal in tumors.

Comparison between MRI Signal Enhancement and Pathologic Findings

To understand the underlying mechanism of heterogeneous contrast enhancement within the tumors by the

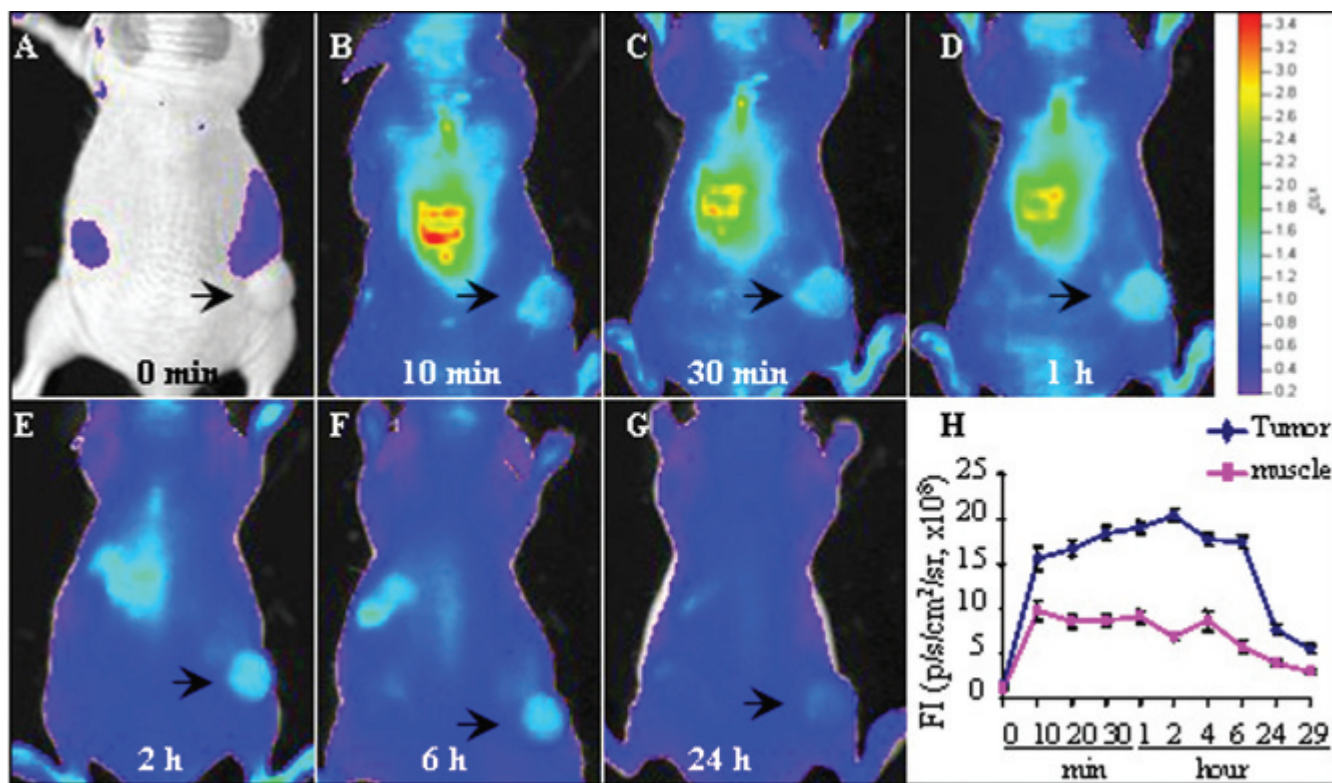


Figure 5. Optical imaging of the tumor after intravenous administration of transferrin-liposome-nitrobenzoxadiazole-contrast agent (Tf^{NIR}-Lip^{NBD}-CA) showing preferential accumulation of fluorescent signal in tumors (A–G). The fluorescence signal was detectable as early as 10 minutes and reached a maximum at about 2 hours and then decreased gradually. H shows the plot of time versus signal intensity obtained from the tumor and the contralateral muscle. The signal intensity is expressed as p/s/cm²/sr.

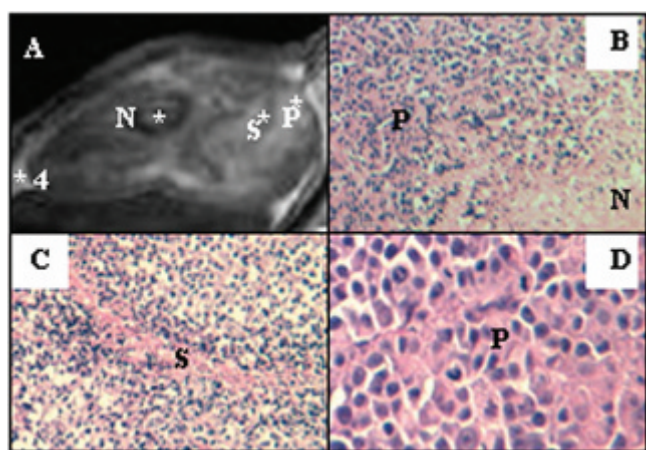


Figure 6. Correlation of magnetic resonance imaging (MRI) with pathologic findings showing high consistency between the probe-mediated enhancement pattern in MRI and pathologic findings (hematoxylin-eosin stain). A is a representative MRI (same as Figure 3) showing a heterogeneous enhancement pattern. B shows a region with high proliferation and necrosis ($\times 250$ original magnification). C shows the stromal tissue ($\times 250$ original magnification), and D shows the proliferating tumor cells with high mitotic activity ($\times 400$ original magnification). N = necrosis; P = proliferating cells; S = stromal tissue.

probe, a comparative analysis was performed between MRI signal enhancement and pathologic findings (Figure 6). Pathologically, the tumor cells in large tumors with heterogeneous enhancement usually presented various stages of growth and necrosis. In some areas, the tumor cells were completely necrotized and became amorphous and liquefied. In some other regions, the tumor cells showed dying features such as condensed or broken nuclei or only shadow cells remaining. The highly enhanced regions of the tumors in MRIs represented the more actively proliferating tumor cells, whereas the weakly enhanced areas contained less active or dying cells. The completely necrotized region showed the least enhancement. The heterogeneous signal enhancement by the probe was well correlated with the *in vivo* morphologic features of the tumors.

Discussion

The human Tf-targeted cationic Lip—deoxyribonucleic acid (DNA) complex has been used for efficient gene

transfer in animal models recently. The formulation for optimal transfection of cancer cells has been optimized as a DNA:lipid:Tf ratio of 1 μ g:10 nmol:12.5 μ g with Lip composition of DOTAP:DOPE (1:1, w/w). This complex of Tf-Lip-DNA demonstrates a highly compact structure that resembles a virus particle with a dense core enveloped by a membrane coated with Tf molecules spiking the surface.^{20,21} Successful gene delivery using Tf-targeted cationic Lip is based on the fact that TfR is overexpressed in various malignant tumors and Tf-TfR-mediated endocytosis is highly efficient. Furthermore, cationic Lip has many advantages, such as high encapsulation capacity, much less immunogenicity and toxicity, and dramatically increased transfection efficiency through linkage with ligands.²² These characteristics of this system also fulfill the criteria for an ideal system for molecular imaging in vivo. Using the advantages of this system, we developed the probe with both NIR fluorescence and MRI reporters, which is suitable for both optical and nuclear MRI.

Use of the NIR fluorescence molecule minimizes the autofluorescence interference from healthy tissue and allows the visualization of tissues millimeters in depth because of efficient penetration of photons in the NIR range.^{11,12} To encapsulate the CA, we directly hydrated the dried Lip films with concentrated CA solution and downsized the Lip-CA complex by sonication and repeated passing through the membrane before linkage with Tf. The Lip:Tf ratio (10:12.5) used in the probe was optimized as reported previously.^{20–24} The dosage of Magnevist was 0.2 mmol/kg, corresponding to two times the recommended dose for the patient. For this amount of Magnevist (even threefold more), almost all of the Magnevist was found to be encapsulated within the Lip, as estimated by gel filtration and fluorescence study. Our previous study also confirmed Magnevist encapsulation within Lip using scanning electron microscopy and scanning probe microscopy.²⁵ The Tf, cationic Lip, and Gd complex was coupled through charge interaction, which makes the preparation of the probe simple enough to be freshly prepared before use. A concern for Lip carrier, as in the gene delivery, is its size. It has been reported that linkage with Tf condenses the Lip-DNA complex with a uniform size of 50 to 90 nm.^{20,23} After sonication of the probe, we found that repeated passing through 200 and 100 nm polycarbonate membranes resulted only in a loss of less than 10% of the probe and the majority of the probe particles were within 100 nm in size based on the fluorescence measurement of the probe. Transportation of the probe across tumor vessels occurs via open gaps, vesicular vacuoles, and/or fenestrations. A characteristic pore cutoff size is measured

ranging from 200 nm to 1.2 μ m in tumors.²⁶ Another analysis points out that the pore cutoff size is around 400 nm based on in vivo fluorescence microscopy studies of the transportation of sterically stabilized Lip into solid tumors.²⁷ Therefore, the size of our probe should not be a limitation to transport from tumor vasculature into tumor cells.

We first evaluated the probe-mediated uptake efficiency of the reporters in vitro. To visualize and quantify the efficiency, the components of the probe were differentially labeled. On confocal microscopy, Tf^{NIR}, Lip^{NBD}, and the encapsulated NIR dye were clearly codistributed within the cytoplasm of tumor cells. They accumulated and formed endosomes again in the peripheral area of the cytoplasm. In Tf-Lip-mediated plasmid DNA transfection, similar endosome formation has been reported by Lee and Kim.²⁸ They also found nuclear localization of the Tf-Lip. In our system, no nuclear signal of the probe was observed. Quantitative analysis using optical imaging further confirmed the finding of confocal microscopy. The cellular uptake was mediated by both Tf and Lip. Blockage of the TfR with Tf led to significantly decreased uptake. The possibility of nonspecific binding to free NIR dye was excluded because no fluorescent signal of the dye was detected in cells incubated with dye alone. Higher cellular uptake of the Lip and dye in cells incubated with Lip^{NBD}-dye without Tf linkage than in cells incubated with dye alone is not surprising. The probe reporters are taken up in vitro by two different pathways. One is due to Lip-mediated endocytosis and membrane fusion process because Lip is an effective transfection reagent.²² The other is due to binding to TfR. The pretreatment with Tf is not expected to prevent endocytosis of the probe reporters owing to Lip fusion with the cell membrane. Importantly, Tf and Lip showed a synergistic effect on the probe uptake by cells based on our quantitative and blocking analysis. MRI of the cell pellets revealed a similar finding that CA is internalized and the internalization is mediated by both Tf and Lip. The apparent synergistic effect may be explained by a three-step mechanism. The important first step is the specific binding of Tf with TfR on the cell surface followed by the interaction of cationic Lip with anionic cell membrane and finally the receptor- and Lip-membrane fusion-mediated endocytosis.²⁹

For MRI study, a T₁-weighted imaging technique was used to evaluate the positive contrast enhancement mediated by our probe. The actual T₁ shortening in vivo depends on the accumulation of the probe in time, which, in turn, depends on tumor physiology. We have searched the best imaging strategy by using different imaging

sequences and by varying the imaging parameters. The choice of SE sequence with TR = 800 milliseconds and TE = 11.4 milliseconds was based on the consideration of overall image quality, imaging time, and the differences of contrast enhancement between the probe and CA-alone studies. Consistent with our *in vitro* findings, specific targeting of the probe *in vivo* was demonstrated by both optical imaging and MRI. A preferential accumulation of the fluorescent signal in tumors and a significant signal enhancement are clearly achieved with the dual probe but not with CA alone. Time course study revealed a high consistency among confocal images, optical fluorescence, and MRI contrast enhancement. The maximum signal enhancement and FI in tumors are seen at ≈ 90 minutes, and both reach a plateau (which includes the maximum) between 1 and 3 hours after intravenous injection, whereas the maximal magnetic resonance contrast enhancement is achieved at about 45 minutes following administration of CA alone and the enhancement reduces to baseline within 3 hours. The magnetic resonance signal enhancement achieved by the dual probe is much stronger than that achieved by the CA alone. These results are consistent with the finding in gene therapy using a Tf-mediated Lip system that high gene transfection efficiency is observed within tumors.^{23,24} More interestingly, heterogeneous enhancement in MRIs is evident in large tumors, which correlates well with the histologic findings. Within the range of tumor sizes in the present study, CA alone could enhance the image contrast, but the enhancement was weak and relatively uniform. Heterogeneous enhancement that could be correlated with histology may be potentially valuable. It makes it possible to interpret the pathologic features based on specifically enhanced MRI. More information could be provided to the clinician without further invasive procedure of biopsy.^{3,30} *In vivo*, significant uptake of the probe reporters was not observed in the case of Magnevist or fluorescent dye containing Lip without linkage to Tf. This may be explained by the fact that the majority of the Lip accumulated within well-perfused organs, such as the liver, spleen, bone marrow, and lung. The uptake and retention of Magnevist or fluorescent dye containing Lip were very low in tumors. This is in contrast to the uptake of Lip bound to Tf. Positive CA may be superior to the negative CA, such as an iron oxide probe. A decrease in the image intensity by negative CA will complicate interpretation of tumor necrosis and poor expression of target receptors. The advantages of using a superparamagnetic Tf-labeled iron oxide probe are the small size and long-range T_2 effect. Because of the long-range T_2 effect, it requires less compound for a greater image intensity change. Our probe

can be used for optical detection of tumors and is potentially useful for imaging the expression level of TfR and tumor cell growth. These parameters are of great value in predicting the prognosis and treatment selection. This goal can be achieved by measuring the intensity of fluorescence in optical images. However, limited penetration of fluorescence is still a problem, particularly for deep organ tumors. Clearly, use of multimodality reporter constructs can overcome many of the shortcomings of each modality alone.^{14,15}

In conclusion, we have described a novel nano-sized molecular probe with both optical and MRI reporters. *In vitro* and *in vivo* analysis confirmed the probe specificity, internalizing efficiency, and sufficiency for multimodality detection. In MRI, the probe significantly enhances the tumor contrast so that it can increase the sensitivity to detect small tumors. The tumor enhancement pattern could help evaluate the pathologic features of tumors *in vivo*, which provides more information for the clinician. Preferential accumulation of the probe NIR fluorescence makes the tumor detectable using NIR-based optical imaging. Furthermore, it provides the possibility of quantifying the specific biomarkers expressed in tumors, which will be helpful to determine the patient's prognosis and response to treatment.

Acknowledgments

We thank Dr. Elizabeth G. Snyderwine and Dr. Minshu Yu (Laboratory of Experimental Carcinogenesis, National Cancer Institute [NCI], NIH) for their scientific advice. We are grateful to Stephen M. Wincovitch and Susan H. Garfield (CCR Confocal Microscopy Core Facility, NCI, NIH) for help and consultation with confocal microscopy.

References

1. Pautler RG. Mouse MRI: concepts and applications in physiology. *Physiology* 2004;19:168–75.
2. Artemov D. Molecular magnetic resonance imaging with targeted contrast agent. *J Cell Biochem* 2003;90:518–24.
3. Massoud TF, Gambhir SS. Molecular imaging in living subjects: seeing fundamental biological processes in a new light. *Gene Dev* 2003;17:545–80.
4. Persigehl T, Heindel W, Bremer C. MR and optical approaches to molecular imaging. *Abdom Imaging* 2005;30:342–54.
5. Blasberg RG. Molecular imaging and cancer. *Mol Cancer Ther* 2003;2:335–45.
6. Funovics MA, Kapeller B, Hoeller C, et al. MR imaging of the her2/neu and 9.2.27 tumor antigens using immunospecific contrast agents. *Magn Reson Imaging* 2004;22:843–50.

7. Basilion JP. Current and future technologies for breast cancer imaging. *Breast Cancer Res* 2001;3:14–6.
8. Artemov D, Mori N, Okollie B, Bhujwala ZM. MR molecular imaging of HER-2/neu receptor in breast cancer cells using targeted iron oxide nanoparticles. *Magn Reson Med* 2003;49:403–8.
9. Mulder WJM, Strijkers GJ, Griffioen AW, et al. A liposomal system for contrast-enhanced magnetic resonance imaging of molecular targets. *Bioconjugate Chem* 2004;15:799–806.
10. Graves EE, Weissleder R, Ntziachristos V. Fluorescence molecular imaging of small animal tumor models. *Curr Mol Med* 2004;4:419–30.
11. Ntziachristos V, Bremer C, Weissleder R. Fluorescence imaging with near-infrared light: new technological advances that enable in vivo molecular imaging. *Eur Radiol* 2003;13:195–208.
12. Hoffman RM. The multiple uses of fluorescent proteins to visualize cancer in vivo. *Nature* 2005;5:796–806.
13. Schellenberger EA, Sosnovik D, Weissleder R, Josephson L. Magneto/optical annexin V, a multimodal protein. *Bioconjugate Chem* 2004;15:1062–7.
14. Blasberg RG. In vivo molecular-genetic imaging: multi-modality nuclear and optical combinations. *Nucl Med Biol* 2003;30:879–88.
15. Veisheh O, Sun C, Gunn J, et al. Optical and MRI multifunctional nanoprobe for targeting gliomas. *Nano Lett* 2005;5:1003–8.
16. Jones DT, Trowbridge IS, Harris AL. Effects of transferrin receptor blockade on cancer cell proliferation and hypoxia-inducible factor function and their differential regulation by ascorbate. *Cancer Res* 2006;66:2749–56.
17. Hogemann-Savellano D, Bos E, Blondet C, et al. The transferrin receptor: a potential molecular imaging marker for human cancer. *Neoplasia* 2003;5:495–506.
18. Xu L, Pirolo KF, Tang WH, et al. Transferrin-liposome-mediated systemic p53 gene therapy in combination with radiation results in regression of human head and neck cancer xenographs. *Hum Gene Ther* 1999;10:2941–52.
19. Bellocq NC, Pun SH, Jensen GS, Davis ME. Transferrin-containing, cyclodextrin polymer-based particles for tumor-targeted gene delivery. *Bioconjugate Chem* 2003;14:1122–32.
20. Xu L, Frederik P, Pirolo KF, et al. Self-assembly of a virus-mimicking nanostructure system for efficient tumor-targeted gene delivery. *Hum Gene Ther* 2002;13:469–81.
21. Kursa M, Walker GF, Roessler V, et al. Novel shielded transferrin-polyethylene glycol-polyethylenimine/DNA complexes for systemic tumor-targeted gene transfer. *Bioconjugate Chem* 2003;14:222–31.
22. Simoes S, Pires P, Duzgunes N, Pedrosa de Lima M. Cationic liposomes as gene transfer vectors: barriers to successful application in gene therapy. *Curr Opin Mol Theory* 1999;1:147–57.
23. Nakase M, Inui M, Okumura K, et al. p53 gene therapy of human osteosarcoma using a transferrin-modified cationic liposome. *Mol Cancer Ther* 2005;4:625–31.
24. Pirolo KF, Xu L, Chang EH. Non-viral gene delivery for p53. *Curr Opin Mol Ther* 2002;2:168–75.
25. Pirolo K, Dagata J, Wang P, et al. A tumor-targeted nanodelivery system to improve early MRI detection of cancer. *Mol Imaging* 2006;5:41–52.
26. Hobbs SK, Monsky WL, Yuan F, et al. Regulation of transport pathways in tumor vessels: role of tumor type and microenvironment. *Proc Natl Acad Sci U S A* 1998;95:4607–12.
27. Unezaki S, Maruyama K, Hosoda JI, et al. Direct measurement of extravasation of poly-ethyleneglycol-coated liposomes into solid tumor tissue by in vivo fluorescence microscopy. *Int J Pharm* 1996;144:11–7.
28. Lee SM, Kim JS. Intracellular trafficking of transferrin-conjugated liposome/DNA complexes by confocal microscopy. *Arch Pharm Res* 2005;28:93–9.
29. Yin J, Lin AJ, Buckett PD, et al. Single-cell FRET imaging of transferrin receptor trafficking dynamics by sfp-catalyzed, site-specific protein labeling. *Chem Biol* 2005;12:999–1006.
30. Mankoff D. Imaging in breast cancer—breast cancer imaging revisited. *Breast Cancer Res* 2005;7:276–8.